Bull. Min. Res. Exp. (2016) 152:121-141

BULLETIN OF THE
MINERAL RESEARCH AND EXPLORATION

http://bulletin.mta.gov.tr

AN APPROACH TO THE ORIGIN OF THE EARLY CAMBRIAN KARAÇAT IRON DEPOSIT (MANSURLU BASIN, ADANA) AND IRON DEPOSITS OUTCROPS AT ITS EASTERN PARTS

Deniz TİRİNGA[a]*, Taner ÜNLÜ[b] and Semih GÜRSU[c]

[a]*General Directorate of Mineral Research and Exploration (MTA), Department of Mineral Research and Exploration, Ankara, Turkey*

[b]*Ankara University, Department of Geological Engineering, Ankara, Turkey*

[c]*Muğla Sıtkı Koçman University, Department of Geological Engineering, Muğla, Turkey*

Research Article

Keywords:
Iron Mineralization, Karaçat Iron Deposit, Mansurlu, Exhalative Syn-Sedimentary.

Received: 09.11.2015
Accepted:27.11.2015

ABSTRACT

The Neoproterozoic basement and the Early Cambrian units are widely exposed around the Karaçat Iron Deposit and its surrounding, which are located at the eastern part of Tauride-Anatolide platform. The main mineralization was detected as hematite in all deposits in the study area. The ore microscopy, SEM and EDX studies show that carbonate pseudomorphs in hematite have developed and their chemical compositions are enriched in Ca, Mg, Fe, C and O elements. The geochemical analyses of hematite and siderite minerals reveal that both ore mineral types have similar patterns of Rare Earth Element (REE). These data and field observations reveal that hematite is the replacement product after sedimentary siderite mineralization. The genesis of the hematite mineralization that is effective over large areas and widely observed on the basement and overlying units, was formed during Late Neoproterozoic- Early Cambrian volcanism in the region defined as Peri-Gondwana. They are genetically described as volcano syn-sedimentary and/or exhalative syn-sedimentary type mineralization.

1. Introduction

Different types of economic ore mineralizations have been developed in our country located along a belt that was actively affected by Pan-African, Cadomian, Variscan and Alpine orogeneses. Iron deposits formed one of these mineralizations has been observed in the different basins indicating different genesis, ages and lithologies (Cihnioğlu et al., 1994).

Mansurlu Basin iron deposits are observed within the siliciclastic rocks of the Late Proterozoic-Early Cambrian. Similar formations in the Precambrian shields in North and South America, Africa, Australia and Russia are shortly defined as Banded Iron formations (BIF). The BIFs form significant portion of iron ore deposits in the whole world. The Mansurlu basin is the second biggest iron deposit in terms of reserve in our country. Iron deposits and occurrences, located at the eastern part of Mansurlu Basin, host good quality direct reduced iron ores in their bodies for blast furnaces. They contain 65 % Fe content as tenure and do not include any harmful compound.

Among deposits in the basin, several studies were carried out to reveal the formation of iron deposits in Attepe and its close vicinity (Lucius, 1927; Brennich, 1961; Arıkan, 1966, 1968; Henden et al., 1978; Önder and Şahin, 1979; Henden and Önder, 1980; Ünlü et al., 1984; Ünlü, 2003; Küpeli, 1986; 1991 and 1998; Ünlü and Stendal, 1986, 1989; Dağlıoğlu and Bahçeci, 1992; Dağlıoğlu et al., 1998; Çolakoğlu and Kuru, 2002; Küpeli et al., 2006; Dayan, 2007; Arda et al., 2008; Dayan et al., 2008; Tiringa, 2009; Tiringa et al., 2009, 2011).

The genesis of the iron deposits in the studied area is not well known though some researchers proposed hydrothermal-type genesis (related to the granitic intrusions) as their possible provenance

*Corresponding author:Deniz TİRİNGA, deniz.tiringa@mta.gov.tr
http://dx.doi.org/10.19111/bmre.16543

(Henden and Önder, 1980; Küpeli, 1991; Küpeli et al., 2006). However; the other researchers mentioned that primary iron mineralizations were formed from siderites in the graphitic schists of the Precambrian Emirgazi formation and from sedimentary hematite observed in their upper parts and from sedimentary pyrites showing disseminated and conformal bedding relationships within the graphitic schists (Küpeli, 1991; Dağlıoğlu et al., 1998; Arda et al., 2008; Dayan, 2007; Dayan et al., 2008; Tiringa, 2009; Tiringa et al., 2009). Some of the researches (Dayan et al., 2008; Tiringa et al., 2009, 2011) provided evidence for volcano syn-sedimentary and/or exhalative syn-sedimentary type genesis models for their occurrences.

The aim of the study is to determine the origin of the iron deposits observed in the Mansurlu basin by field studies, tectonic evolution modelling and petrogenetic studies.

2. Geology of the Study Area

The study area represents characteristic features of the Eastern Taurides in the Tauride-Anatolide platform (Özgül, 1976; 1983; Göncüoğlu, 2010). It is located in the southeastern part of the central Anatolia region between Karaköy village of Yahyalı Town in Kayseri and Bahçecik and Bekirhacılı villages of Feke town in Adana. The geological map of this area is given in figure 1a.

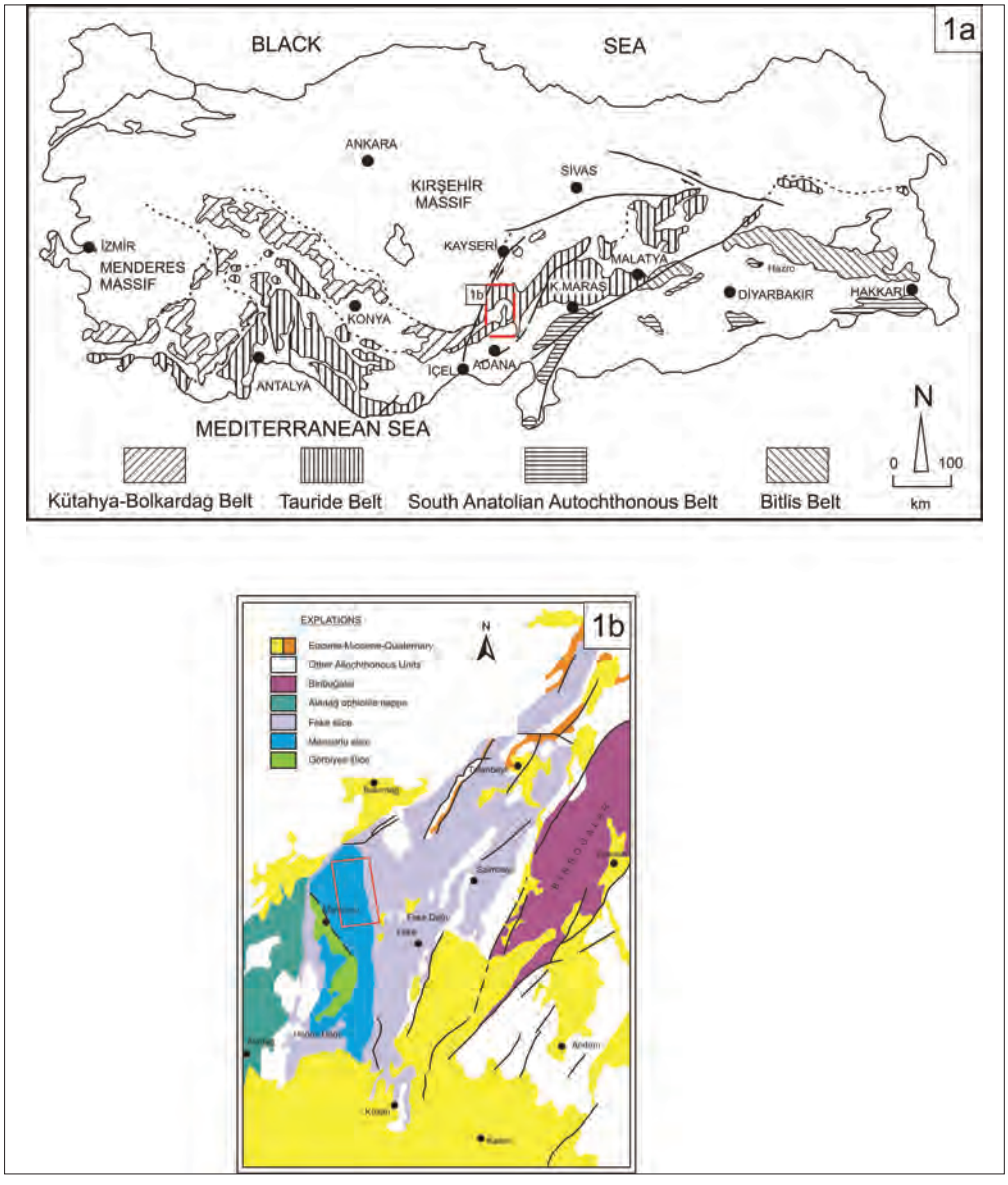

Figure 1- (a) Tectonic terranes of the Southern Anatolites (Göncüoğlu et al., 1997), (b) Studied area and tectonic slices of the Geyikdağı Unit (adapted from Şenel et al., 2004).

In the study area, diverse tectonic slices were described as Görbiyes, Mansurlu and Feke indicating different stratigraphic and tectonic settings assessed within the Geyikdağı unit (Özgül and Kozlu, 2002; Şenel et al., 2004) (Figure 1b). The allochthonous Görbiyes tectonic slice located at the basement in the region is tectonically overlain by Mansurlu slice. Feke slice, which is formed from different rock groups between the Late Proterozoic-Late Cretaceous, tectonically overlies Mansurlu slice in the studied area. The studied area is located within the Mansurlu tectonic slice (Özgül and Kozlu, 2002) and partly interpolates with the rocks of the Feke slice (Figure 1b).

The Late Neoproterozoic-Early Ordovician rock units in the Mansurlu tectonic slices are cropped out in the studied area (Figure 2). The base unit of the Mansurlu slice is composed of the Emirgazi formation representing the oldest lithostratigraphic unit of the region and is made up of shallow siliciclastics as meta-siltstone and meta-mudstone with meta-volcanic and meta-carbonate interlayers associated with meta-clastics.

The Early Cambrian Koçyazı formation is composed of graphite schist and meta-siltstones/meta-sandstones with meta-mudstones/meta-siltstones inlayers. Mafic volcanic rocks and dykes are observed at lower parts of the formation (Özgül and Kozlu, 2002).

The Zabuk formation, which is intercalated with sandstones and slates in the lower layers, is mainly composed of quartzite (quartz arenites).

The Middle Cambrian Değirmentaş formation is mainly composed of neritic carbonates (Özgül and Kozlu, 2002).

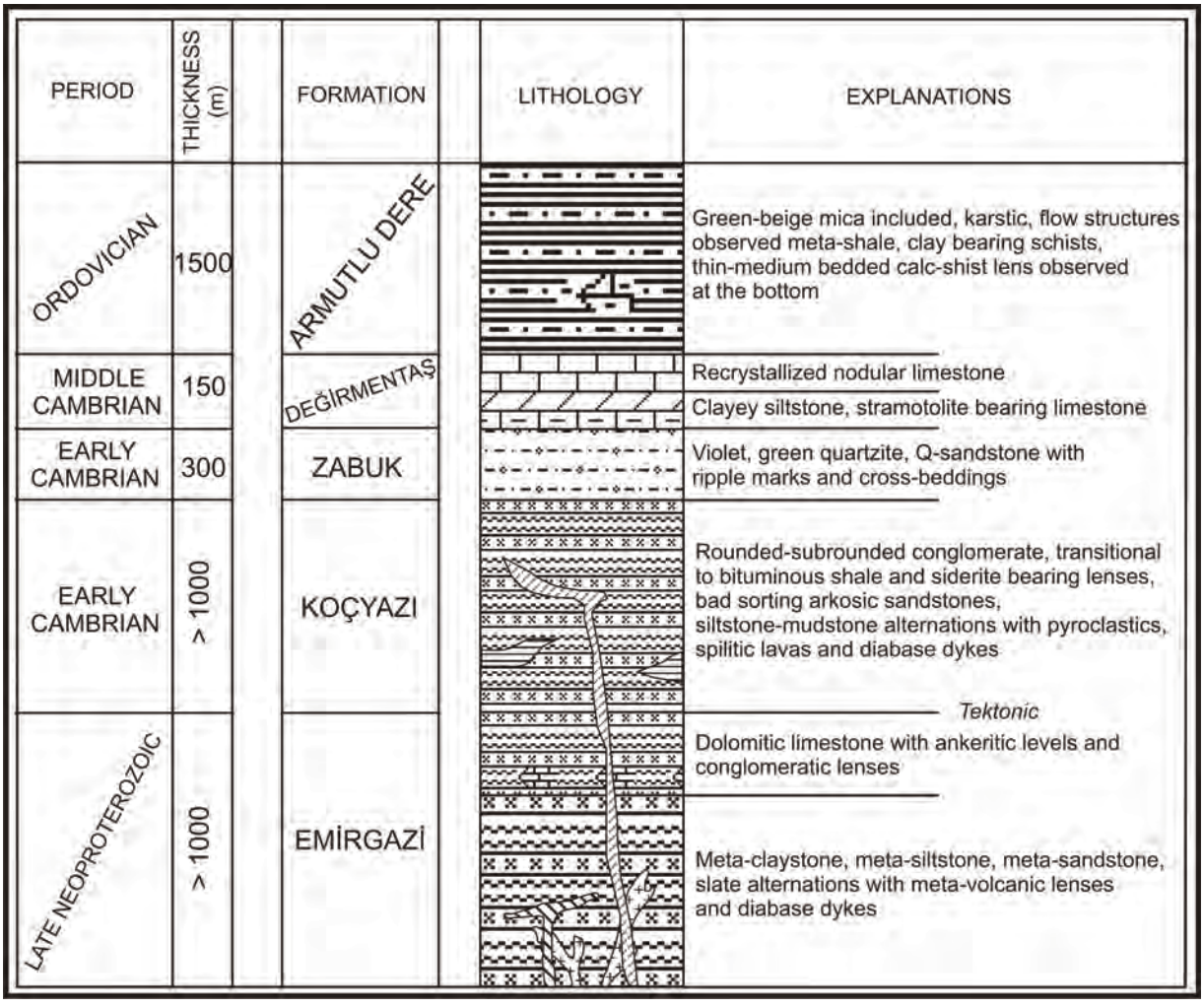

Figure 2- Generalized columnar section of the Mansurlu slice in the studied area (modified from Özgül and Kozlu, 2002).

The Armutludere formation (Demirtaşlı, 1967) is composed of Late Cambrian-Early Ordovician siliciclastic rocks. The folded nodular limestone layers and rare quartz arenite intercalations are observed in the lower part of the succession.

Iron deposits and mineralizations in the Mansurlu basin are stratigraphically observed in the successions from the Late Neoproterozoic Emirgazi formation to Ordovician Armutludere formation. However, no mineralization is observed in the younger successions in the studied area (Figure 3).

2.1. Emirgazi Formation (Late Proterozoic)

Outcrops of the Late Neoproterozoic Emirgazi formation in the basement are located in Üçtepeler within the eastern part of Bahçecik creek, Gökbelen Hill near Hıdıruşağı village, Yüksün Hill, Bekirhacılı village and southern part of Hıdırusağı village (Figure 3).

The main lithology of the Emirgazi formation consists of alternation of meta-sandstone, meta-siltstone with meta-tuff, meta-volcanite, ankerite and meta-carbonate inlayers. The acidic and intermediate felsic volcanic rocks are rarely observed in the succession. The quartzitic rocks are dominant in the upper part of the formation and continue with the recrystallized limestones, dolomitic limestones, dolomites and meta-clastic rocks. Limestones in the upper part of the formation are generally pale to dark ash, yellowish-gray, fine to medium bedded and fine to medium crystallized.

Randomly specularite bearing reddish-brown color carbonate layers that turn into ankerite, lens shaped dolomite and dolomitic limestone layers having 1-10 m thickness are frequently observed in the Emirgazi formation (Özgül and Kozlu, 2002) (Figure 4).

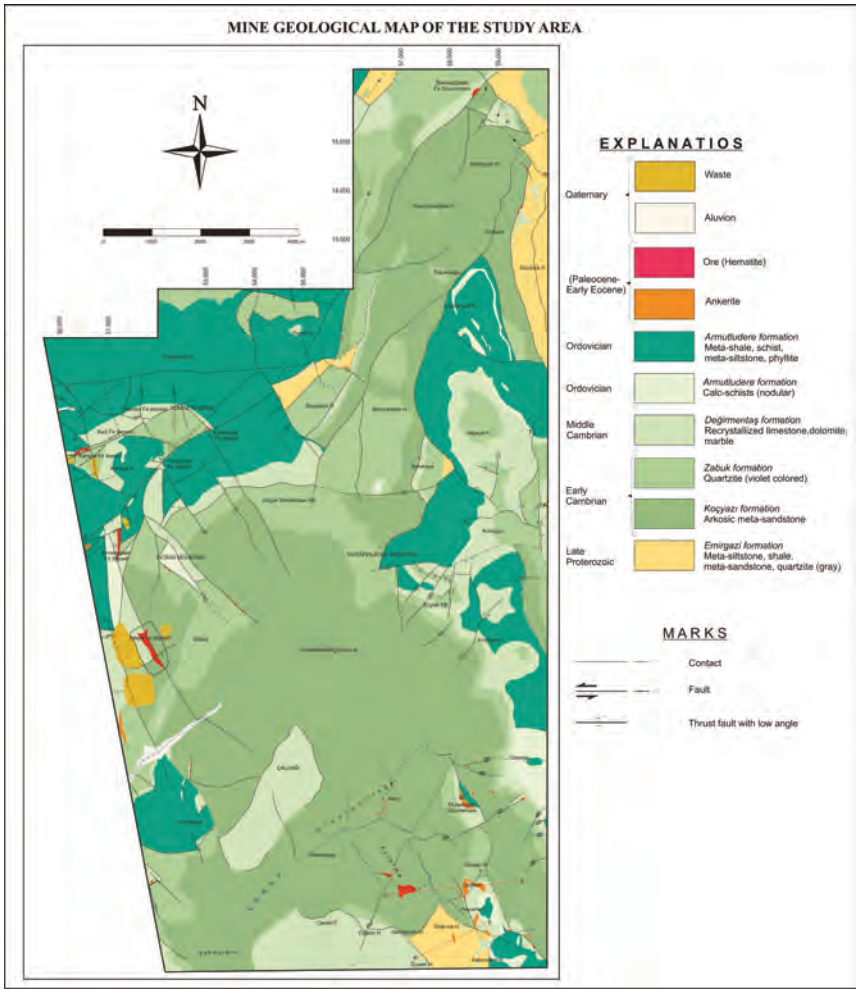

Figure 3- The map of the ore geology in the studied area (adapted from Tiringa et al., 2011).

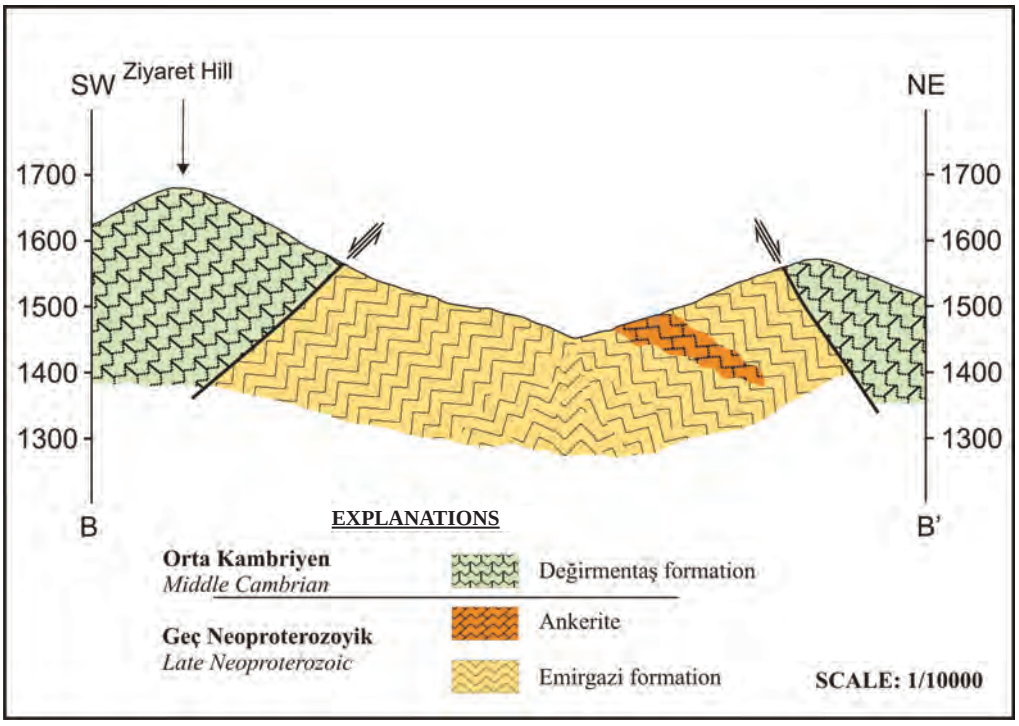

Figure 4- Cross section of the Emirgazi formation showing the ankeric levels at the Ziyaret hill.

In petrographical studies, the ankerites were mainly formed from the different grain sized carbonate minerals that display pressure twinning due to active tectonic deformations. Secondary iron oxide developments are observed along the fractures and cleavage planes of the carbonate minerals. The secondary carbonate minerals are hosted in the pores and fracture zones (Figure 5).

Additionally, limonites formed by the alteration product of ankerite and anhedral dissemine along the outer boundaries with grain size of the 14-240 microns displaying parallel to bedding planes of the host rocks are observed in the samples. It is considered that these iron rich minerals observed in the hand specimens and thin sections were products of the iron deposits in the basin studied as main ore sources.

The formation is adversely affected by the Late Alpine deformation phase having a thickness higher than 1000 meters. The Emirgazi formation is tectonically overlain by the Early Cambrian Koçyazı formation (Özgül and Kozlu, 2002).

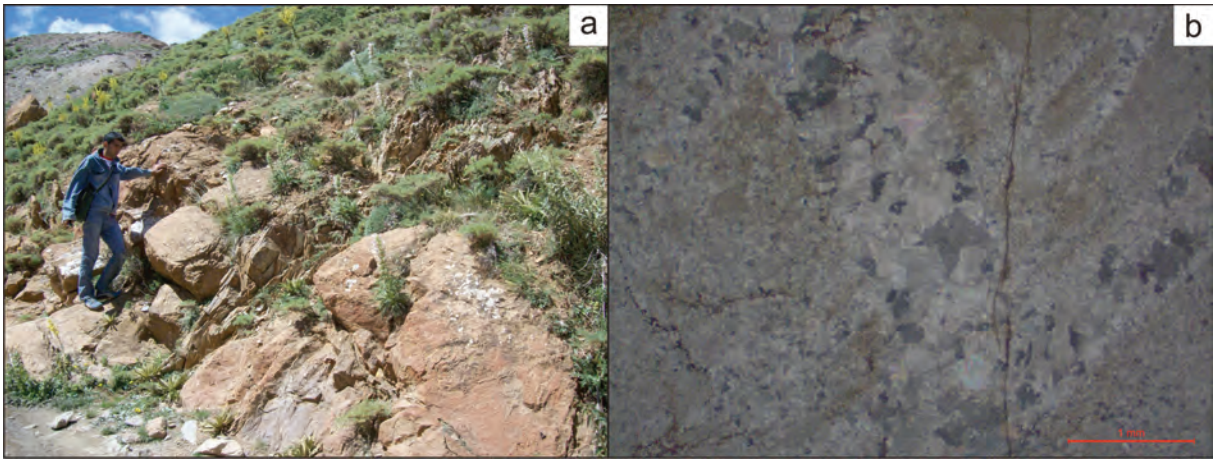

Figure 5- (a) Field photograph of the Ankerite (Menteş dere), (b) photographs of the iron oxides stained ankerite (XPL)

2.2. Koçyazı Formation (Early Cambrian)

The type locality of the formation in the study area is located between Avuç District and Çaldağ. The other outcrops are observed in Küçüktahtafırlatan Hill near the eastern part of Attepe, Şahmuratlı and Kerimuşağı areas of Oruçlu village near the southern part of Yüksün Hill and Kavurmaderesi Hill in the north near the southern part of the Banazlıgedik Hill (Figure 3).

The succession is predominated by meta-sandstone/meta-siltstone. Greyish-black pyrite bearing bituminous shale and sideritic bands are observed in the lower part of the formation (Figure 6a). The type locality of the sideritic bands is placed in NE part of Attepe Iron Deposit at the western part of the study area (Dayan, 2007) (Figure 6b). The basic volcanic rocks are only observed in Karaçam creek in the study area and mark the active basic volcanism at the lower parts of the succession. The upper parts of the succession are composed of fluvial siliciclastic rocks characterized by red-vivid-pink mudstone/siltstone alternations.

The Koçyazı formation is conformably overlain by sandstone-dominated Early Cambrian Zabuk formation that has a continuous succession throughout TAP (Figure 7).

2.3. Zabuk Formation (Early Cambrian)

The outcrops of the formation are placed in Domuztümseği Hill in the northeastern Karaçat Iron Deposit, Tahtafırlatan Mountain, Küçüktahtafırlatan Hill, Kandilcik Hill, Oturum area and Osman Sivrisi Mountain and Bahçecik Village at the west (Figure 3). The unit consists of meta-sandstone dominated slate banded meta-clastic rocks.

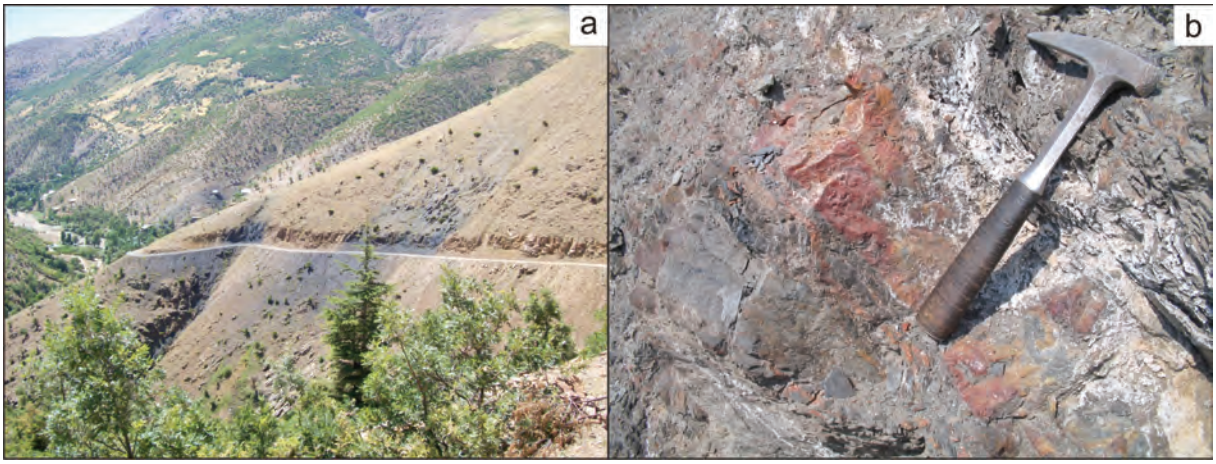

Figure 6- Field photographs (a) Bituminous schist observed at the bottom parts of the formation, (b) siderite lens transitional to the bituminous schist (NE of the Attepe iron deposit).

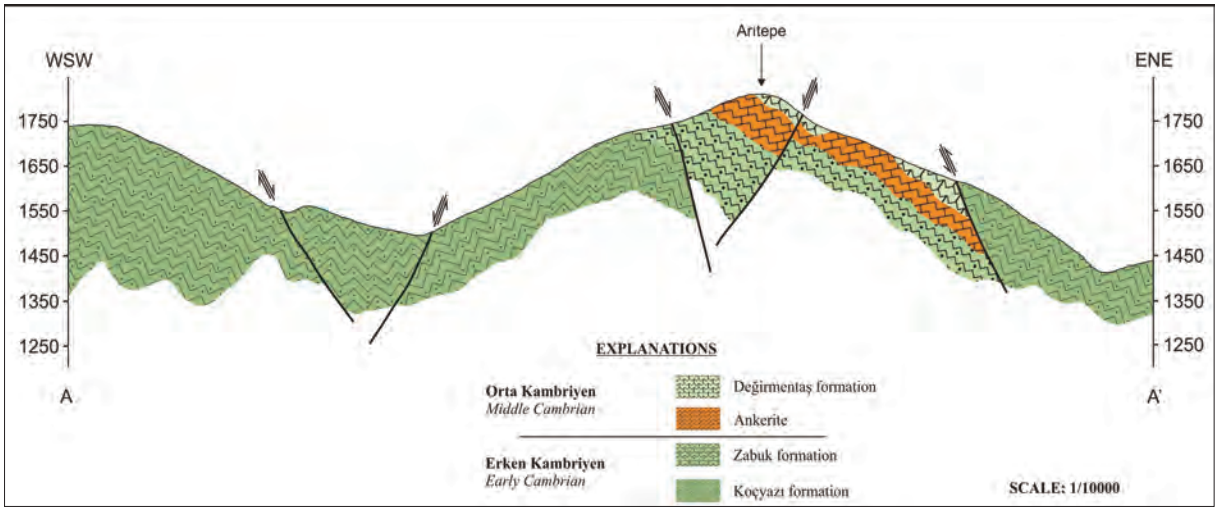

Figure 7- Cross-section showing the transitional contact between Koçyazı formation and Zabuk formation (W of Arıtepe).

The lower part of the formation starts with quartzite and slate intercalation and continues with quartz-sandstone dominated clastic rocks. The angular/sub-angular detritic hematite minerals are observed in the quartzites having 1 to 2 mm grain size. The limonitized, partly specularized hematites and abundant specularites bearing quartz veins are observed in the meta-sandstones (Figure 8). Although there are no economic iron mineralization in the formation, these iron minerals might have been transported to the basin from the land and might have been resulted in the limited precipitation of the iron mineralization.

The unit is conformably overlain by the Middle Cambrian carbonate-dominated Değirmentaş formation (Özgül and Kozlu, 2002).

2.4. Değirmentaş Formation (Middle Cambrian)

The outcrops are best exposed in Osman Sivrisi Mountain, Çaltepe-Oturum areas, and highlands of the northern part of Küçüktahtafırlatan Hill, Karaçat Hill and western part of Bahçecik Village (Figure 3).

The Değirmentaşı formation represented by neritic carbonates is composed of beige, pale brown clay bearing limestones, bluish-gray, gray and dirty white color medium to thick bedded dolomitic limestones and white to beige recrystallized limestones. Abundant calcite-quartz, hematite and siderite mineralization is developed along the fractures and joints of the formation (Figure 9).

Although the formation does not contain primary iron mineralization, a great majority of the second phase iron deposits have been hosted in the formation observed in the Mansurlu basin.

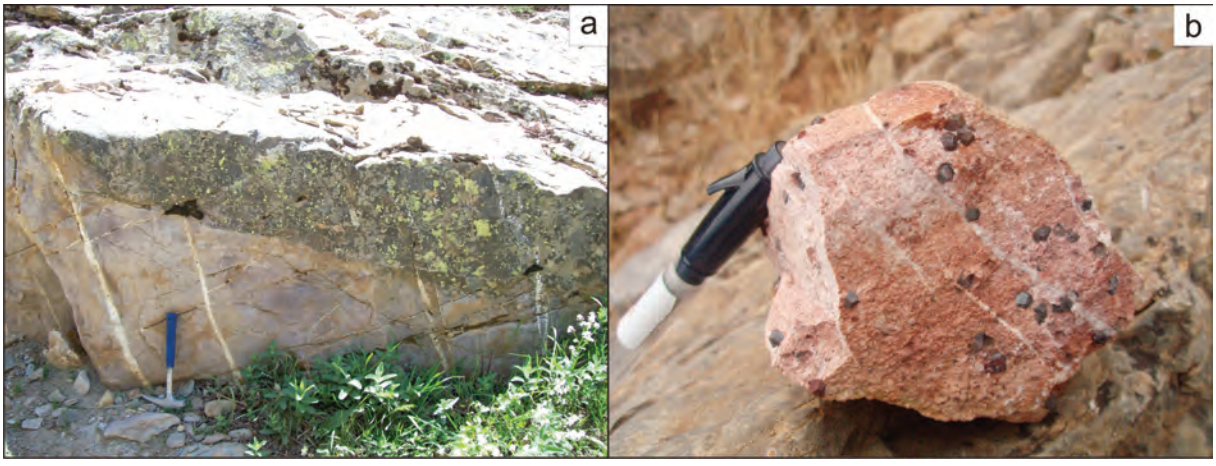

Figure 8- Field photographs; (a) meta-sandstone and quartzites of the Zabuk formation (Menteş dere), (b) detrital hematites deposited together with quartz grains.

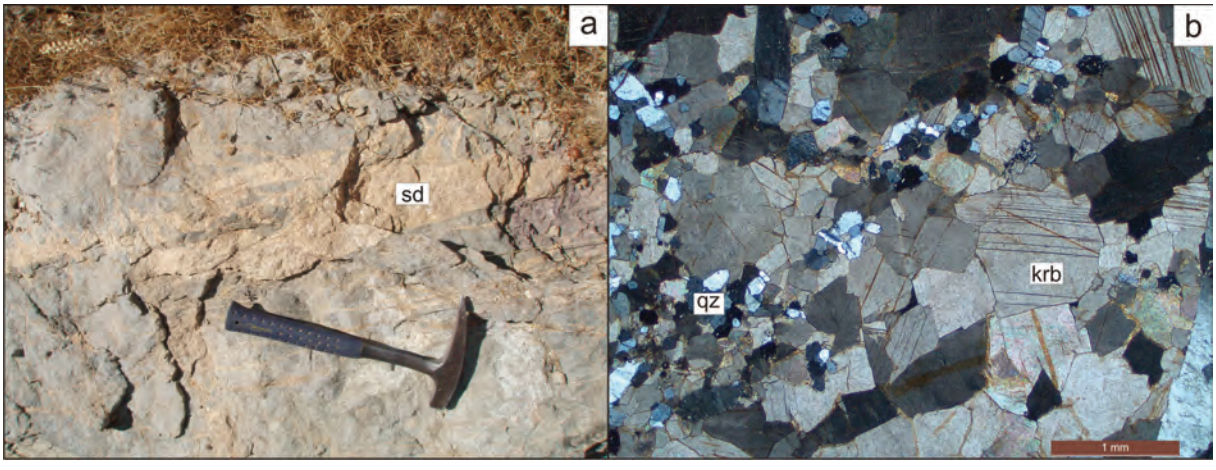

Figure 9- (a) Field photograph of the dolomitic limestone filled with the secondary siderite along the joints and fractures (Kozan-Okçulu area), (b) limonitized carbonates along the clevage planes (sd: siderite, krb: carbonate, qz: quartz).

The settlement of the iron mineralizations in the formation were developed throughout the abundant fractures, faults, karstic spaces within the formation. The dolomitic lithology of the formation displays a convenient porosity for the ore-bearing solutions. Ore tenors after the settlement to the host rocks are extensively enriched by the active secondary processes (Tiringa, 2009; Tiringa et al., 2009, 2011).

The Değirmentaş formation is conformably overlain by nodular limestone layers in the lower parts of the Armutludere formation (Özgül and Kozlu, 2002).

2.5. Armutludere Formation (Late Cambrian-Ordovician)

The outcrops of the formation are observed in the Deveçökeği Hill in the north, Küçüktahtafırlatan Hill and northern hillside of the Sicim Mountain and Uğurunyurt Hill and Atkırı Hill in the west (Figure 3).

The base of the formation starts with beige, pink thin-middle bedded nodular limestone and continues with greenish, pale brown meta-siltstones.

Late-stage hematite mineralization near the lower part of the formation deposited in the calc-shists is widely observed. These mineralizations in the calc-shists lenses are limited as observed as small masses. The siderite lenses (their thickness range from 10 cm to 1-2 m) are observed in southeastern part of the Karaçat Iron Deposits formed in the upper part of the Armutlu formation (Figure 10). 20-30 m thickness of the siderite deposits in the formation is reported from the drilling studies.

The upper part of the Armutludere formation is not observed in the study area and is tectonically overlain by the Late Neoproterozoic Emirgazi formation of the Feke slice.

3. Ore Microscopy Studies

Ore microscopy studies were carried out on 268 samples collected either from ore or from the host rocks representing the mineralization of the different deposits observed in the basin. The results are discussed in the following.

3.1. Precambrian-Early Cambrian Metasiltstones and Basic Rocks

Disseminated magnetites and marcasites were determined by the ore microscopy studies carried out in both of Precambrian and Early Cambrian siltstones. The magnetites are in the form of the euhedral-subhedral rectangle or triangle shape grains that are in different sizes. The martitizations are observed along the weak zones of the magnetites. The ilmenite, rutile and titanites as the forms of the cage structure are main alteration products of the ilmenomagnetite, pyrite (partly altered to goethite, hematite), chromite (partly replaced by magnetite along the weak zones), chalcopyrites and magnetites were determined in the ore microscopy studies of the basic volcanic rocks (Figure 11).

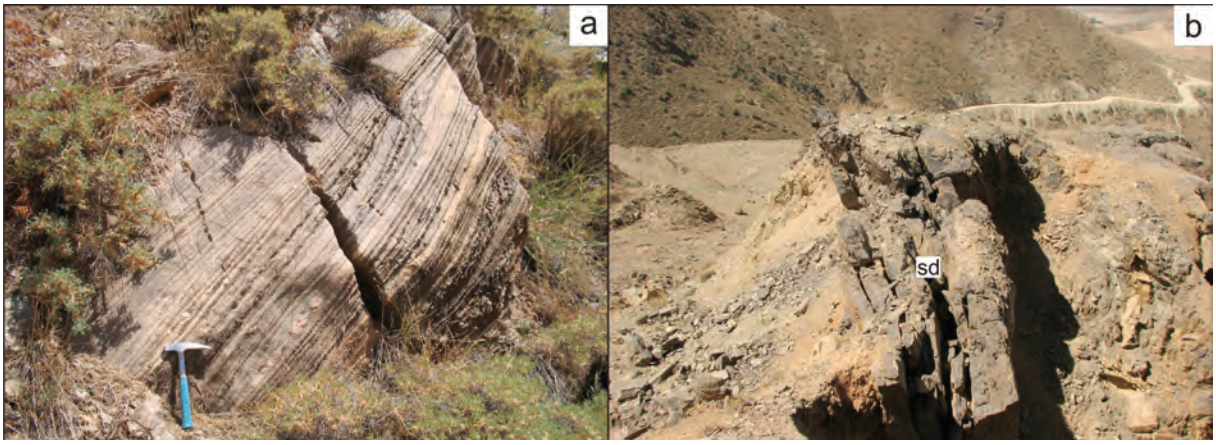

Figure 10- Field photographs; (a) Nodular limestone (NW of Alpseki creek), (b) siderite lens in the meta-siltstone (SE of Karaçat iron deposit) (sd: siderite).

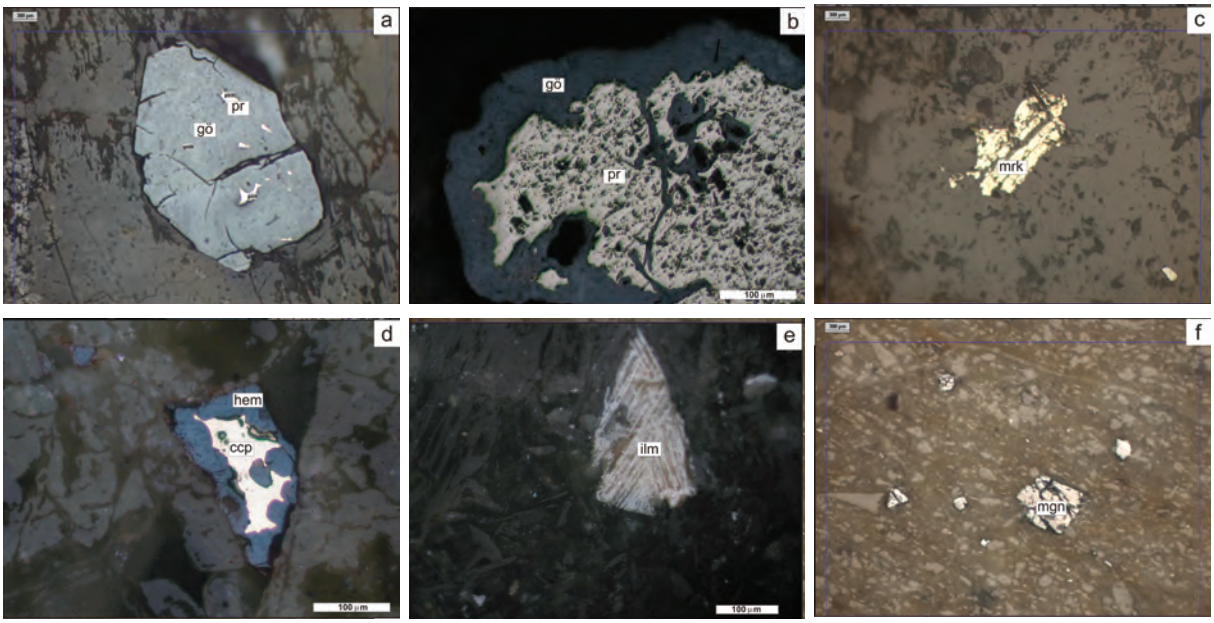

Figure 11- (a) Subhedral, goethite derived from pyrite (b) Goethite derived from pyrite along the cleavage planes (c) Marcasite within the meta-siltstone (d) Chalcopyrites observed within the hematite (e) Ilmenite lamelea (f) Euhedral-subhedral magnetites partly replaced by martitation (pr: pyrite, gö: goethite, ccp: calcopyrite, ilm: ilmenite, hem: hematite, mgn: magnetite, mrk: marcazite)

3.2. Middle Cambrian Limestones

The limonites and limonitic stains are discovered in the Middle Cambrian dolomitic limestones and partly limonitized pyrites along the weak zones and sub-microscopic hematites are developed in the recrystallized limestones during the ore microscopy studies (Figure 12). Variated grain size of the carbonate minerals showing strain twins due to deformation were observed in the petrographic studies. In addition, abundant limonite strains and limonitization were detected throughout cleavage planes, grain boundaries and fractures (Figure 9).

3.3. Specularites

The different grain size of the goethites and specularites observed as lensoidal, detached, folded-bended due to cataclastic effects were determined in the polished sections. The specularites are also offset in some places in the form of rods having different thicknesses that display pronounced alignments. The red internal reflections of the hematites are distinctive in some sections. Specularite mineralization surrounding the goethite ores are tended to fill the cracks and fractures of the ore. Their relationships with host rocks are limited just in settlement into cracks and fractures. No substitution textures or traces in the Middle Cambrian recrystallized limestones are determined (Figure 13).

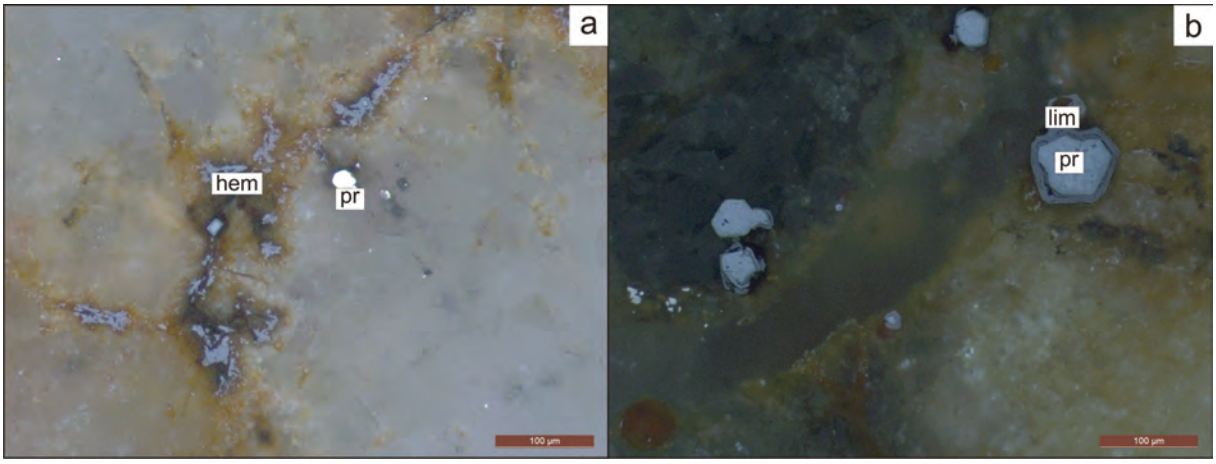

Figure 12- (a) Submicroscopic hematite and euhedral pyrite (b) Euhedral limonitized pyrite along the cleavage planes (hem: hematite, lim: limonite, pr: pyrite)

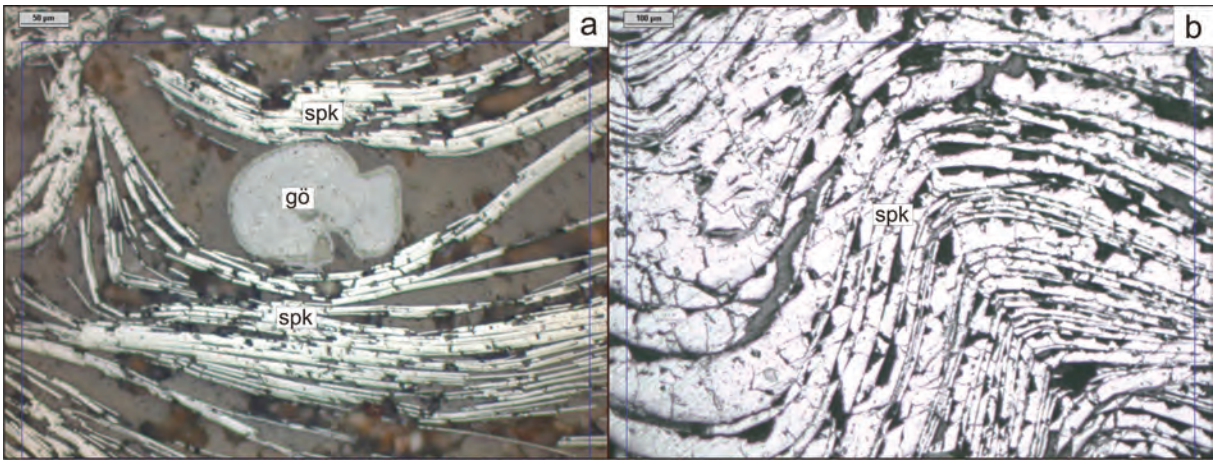

Figure 13- (a) Specularites surrounding the goethite (b) Folding structures in the specularites (spk: specularites, gö: goethite).

3.4. Hematites and Limonites

Abundant hematites and partly pyrite-formed limonites which filled up the cracks and spaces were determined in the polished samples. The hematites and limonites are partly developed as intergrowth grains. The forms of hematites are generally observed as in rhombohedral and sheets having different thicknesses and shows blood to red internal reflections, slightly bended structures with submicroscopic and stain. The typical growing textures identified in the hematites and strain twins lamellae were observed in some sections. The limonitization throughout cracks/ fractures, cleavage planes and grain boundaries were distinctively determined on the hematite mineral.

Limonites were observed as the pseudomorph of the pyrites and stains that filled along the cracks-fractures (Figure 14).

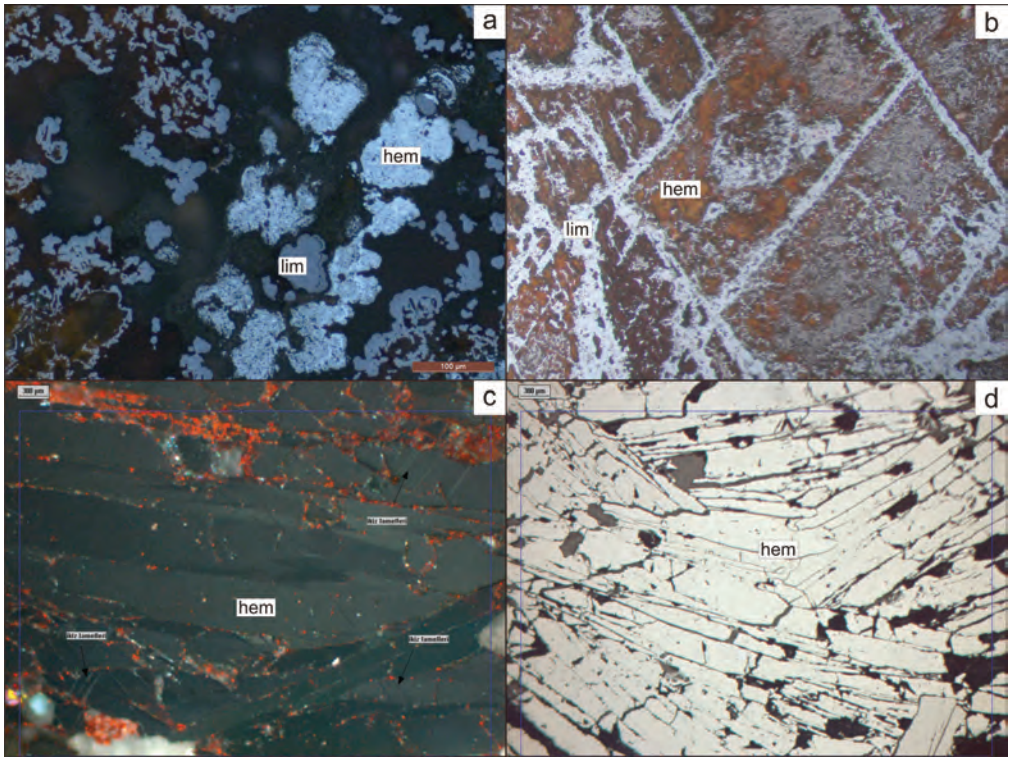

Figure 14- (a) Hematite within limonite (b) Limonitized hematite along the clevage planes and mineral boundaries (c) Twin lamea in the hematite (d) Bended hematite plates (hem: hematite, lim: limonite).

3.5. Siderites

Siderites are the predominant mineral in the genesis of the iron deposits in the basin. Siderite may turn into hematite or magnetite depending on the change of the Eh and pH but may be easily converted to secondary siderite even at low temperatures in supergenetic enrichments (Bubenicek, 1964). In the petrographic studies, the rhombohedral forms as derived by the siderite alteration products in the hematites were determined from the samples taken from the different parts of the basin in the studied area. In this context, the siderites were largely altered to hematites and carbonate minerals or were substituted by hematites and then altered to the limonites along the grain boundaries.

Siderites were mineralogically and petrographically formed from the iron bearing carbonate minerals that showed meso-micro crytalline grain size, cleavage planes, limonitized texture near the boundaries of the grains and strain twins due to the deformation (Figure 15). In addition, the limonites and limonitized strains with rarely subhedral/anhedral limonitized pyrites which occurred along the cleavage planes were observed in the siderite bearing samples (Figure 16).

4. SEM Studies

The ore microscopy studies on the hematite minerals showed that they have carbonate forms. Thus, SEM/EDX analyses were performed on the carbonate minerals to determine their chemistry. The analyses were done in the Mineralogy-Petrography Laboratory of the Department of Mineral Analysis, MTA using FEI Quanta 400 MK2 SEM instrument with EDAX Genesis XM4i EDS detector. The selected polished samples were prepared and coated with carbon before analyses.

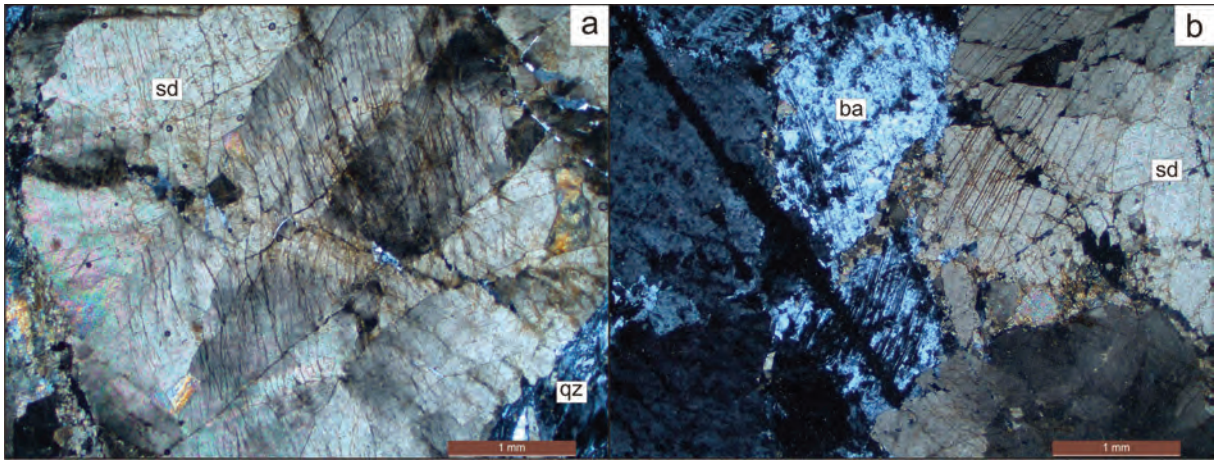

Figure 15- Microphotographs of the siderites, (a) limonitized siderites along the cleavage planes, (b) barite mineral associated with siderites (sd: siderite, qz: quartz, ba: barite).

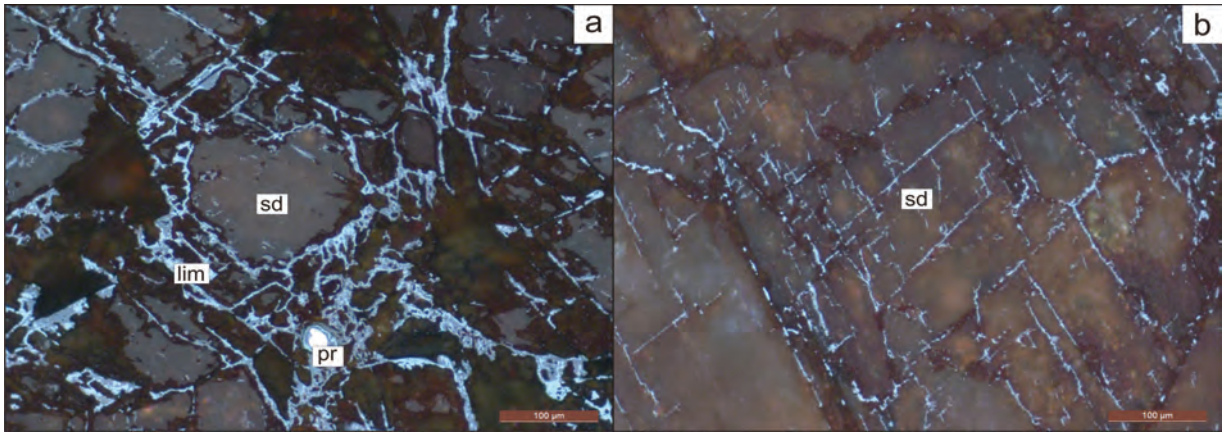

Figure 16- (a) limonitized siderites and pyrite minerals observed in the boundaries and fractures, (b) limonitized siderites along cleavage planes, (lim: limonite, sd: siderite, pr: pyrite)

The elemental analyses were carried out on the 25 spots of the samples by getting their back scatter electron and secondary electron signal images.

The elements Fe, Ca, Mg and Mn were primarily detected in the darker minerals than iron oxides minerals in the polished samples (Figure 17). S, K, Si and Al elements in these minerals were also detected. These elemental patterns clearly reveal that the host mineral associated with hematites is composed of siderite. It is known that Mn, Mg, P, Ca, Zn and Co elements are observed in their chemistry, although their chemical formula are $FeCO_3$. These data show that the carbonate forms observed within the hematites in the polished samples were composed of siderites and hematite formed by the alteration products of the siderites.

5. Geochemistry

A total of 89 samples (78 of which are hematite-goethite and 11 siderite) were collected and analyzed from the core drillings operated by MTA from open pit areas of Karaçat iron deposit, Taşlıkdere iron deposit, İnniktepe iron deposit, Menteşdere iron deposit, Kartalkaya iron deposit and Attepe iron deposit, Demirçoluğu creek in the north of Karaçat iron deposit and Karaköy village (Table 1). The major oxides and rare earth elements of the hematite-goethite and siderite samples taken from same and different parts of the iron deposits display similar elemental patterns.

The average major oxides, trace and rare earth elements of the studied samples normalized against chondrite (Sun et al., 1980) show that elemental patterns of the hematites-goethites and siderites present similar patterns (Figure 18, 19). These findings show that the ore minerals (hematites and goethites) in the studied area have the same origin and alteration products of the siderites.

6. Ore Type Distributions

The iron mineralizations in the Mansurlu Basin were generated in five different stratigraphical stages from Late Neoproterozoic to Early Ordovician. The iron mineralizations were formed as siderite and/or hematite, magnetite, pyrite and ankerite in the Late Neoproterozoic and Early Cambrian series (1), as siderite and/or hematite in the Early Cambrian quartzites and Middle Cambrian meta-carbonates (2), as hematite and specularite in the Middle Cambrian meta-carbonates (3), as hematite in the calc-schists in the Middle Cambrian meta-carbonates and Late Cambrian-Early Ordovician series (4) and as siderite and/or hematite in the Early Ordovician calc-schist lenses and shales (5) (Figure 20).

The results show that hematite mineralization observed in the iron deposits of the Mansurlu Basin was the primary alteration products of the Late Neoproterozoic-Early Cambrian iron ores.

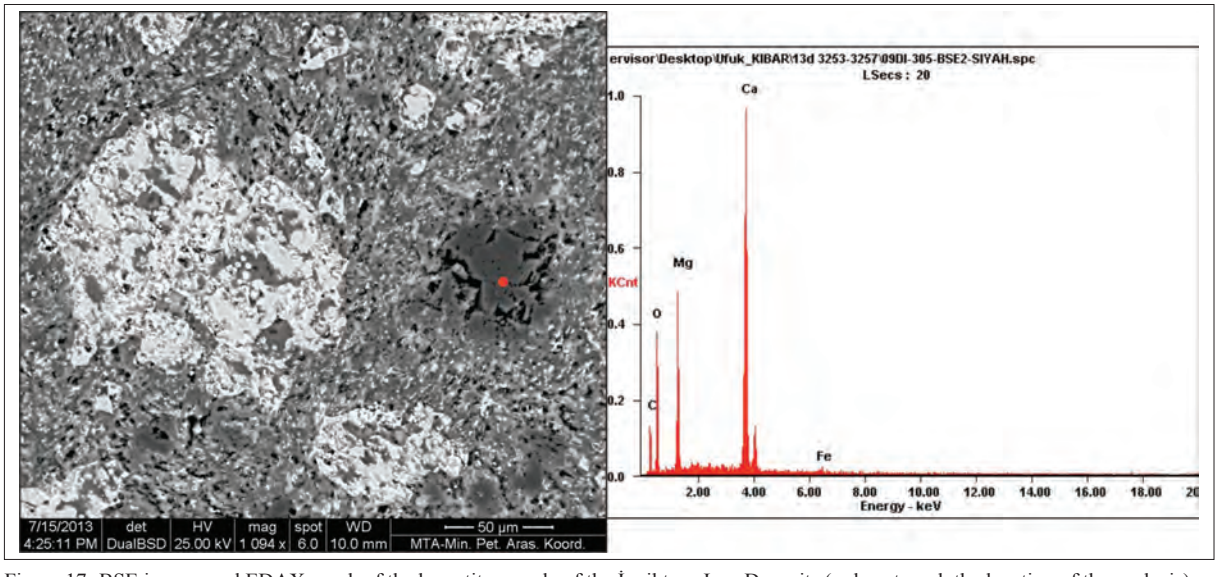

Figure 17- BSE images and EDAX graph of the hematite sample of the İnniktepe Iron Deposits (red spot mark the location of the analysis).

Table 1- Geochemical analyses of the iron deposits in the Mansurlu area (min: mininum value, max: maximum vale, mean: aritmetic mean).

	Karaçat Iron Deposit						Taşlıktepe Iron Deposit						İnniktepe Iron Deposit		
	hematite+goethite n=36			siderite n=4			hematite+goethite n=13			siderite n=6			hematite+goethite n=14		
	min.	max.	mean	min.	max.	mean	min.	max.	mean	min.	max.	mean	min.	max.	mean
%															
SiO_2	0,5	34,8	4,32	0,6	11,5	5,53	1,50	9,30	4,97	2,10	8,40	4,93	0,50	8,10	1,67
TiO_2	0,07	0,1	0,07	0,07	0,07	0,07	0,07	0,07	0,07	0,07	0,07	0,07	0,07	0,07	0,07
Al_2O_3	0,07	1,9	0,21	0,1	0,6	0,28	0,10	1,40	0,60	0,30	1,40	0,77	0,07	0,20	0,10
Fe_2O_3	51,6	94,2	86,42	58,6	64,1	60,20	53,40	82,30	68,23	29,30	53,40	35,40	43,70	84,60	62,79
MnO	0,4	1,7	1,37	0,9	1,2	1,10	0,70	1,70	1,18	0,80	1,20	0,93	0,20	0,70	0,44
MgO	0,07	2,8	0,41	1,3	2,1	1,75	0,20	3,20	1,03	0,30	6,30	1,40	0,20	7,10	1,57
CaO	0,1	6,3	0,86	0,3	0,9	0,55	0,20	16,10	5,28	16,50	32,40	26,47	3,10	24,60	15,41
Na_2O	0,07	0,1	0,07	0,07	0,07	0,07	0,07	0,07	0,07	0,07	0,07	0,07	0,07	0,07	0,07
K_2O	0,07	0,4	0,09	0,07	0,2	0,11	0,07	0,20	0,12	0,07	0,40	0,19	0,07	0,07	0,07
P_2O_5	0,07	0,2	0,07	0,07	0,1	0,08	0,07	0,60	0,12	0,07	0,10	0,08	0,07	0,07	0,07
A.Z.	3,9	16,99	6,16	30	30,8	30,40	10,90	31,40	18,28	24,60	36,80	29,78	10,90	27,70	17,98
ppm															
Ba	6,759	3000	717,87	14	7500	1957,00	50,00	1540,00	464,16	231,14	1000,00	431,63	3,50	119,72	54,85
Rb	0,3	23	4,48	7	7	7,00	0,70	7,00	2,92	0,50	7,00	2,83	0,14	0,90	0,32
Sr	3,5	279	25,47	7	102	54,50	3,50	66,00	8,85	3,50	72,00	15,97	3,50	182,00	22,26
Zr	4	77	10,03	-	-	-	2,00	5,00	3,30	0,35	24,00	12,09	7,00	13,00	9,71
Nb	1	7	3,21	7	14	10,50	1,00	7,00	2,62	0,35	7,00	2,78	0,35	0,35	0,35
Ni	3,5	29	14,44	3,5	11	7,38	41,00	114,00	73,31	21,00	53,00	32,50	13,00	64,00	38,64
Co	4	210	47,89	7	14	10,50	6,00	14,00	9,15	4,00	7,00	5,50	2,00	10,00	7,07
Zn	20,598	89	38,99	30	41	35,50	14,32	29,00	21,20	14,21	43,00	20,29	3,98	26,93	17,28
Cr	3,5	248	17,49	7	21	14,00	3,50	7,00	4,31	3,50	7,00	4,67	3,50	3,50	3,50
La	0,2	7	1,97	7	28	17,50	0,30	7,00	2,75	1,30	7,00	3,35	1,10	4,90	2,35
Ce	0,6	5,9	2,12	-	-	-	0,80	6,20	3,71	3,90	5,00	4,53	1,70	12,00	4,95
Pr	0,1	1	0,39	-	-	-	0,20	1,40	0,81	1,00	1,20	1,10	0,40	2,00	0,86
Nd	0,8	29	7,56	14	19	16,25	1,00	19,00	7,68	5,60	10,00	7,08	2,10	8,20	3,50
Sm	0,4	2,9	1,13	-	-	-	0,50	3,90	2,34	3,00	3,50	3,33	0,80	3,70	1,70
Eu	1	4,4	2,34	-	-	-	0,50	7,20	2,81	2,00	2,70	2,30	0,20	3,60	1,74
Gd	0,5	3,3	1,37	-	-	-	0,80	5,00	3,06	3,60	4,50	4,18	0,60	4,20	2,34
Tb	0,07	0,5	0,22	-	-	-	0,10	0,80	0,45	0,60	0,70	0,65	0,07	0,70	0,38
Dy	0,6	3,1	1,47	-	-	-	0,80	3,90	2,42	3,40	3,80	3,60	0,30	3,20	1,86
Ho	0,2	0,6	0,32	-	-	-	0,20	0,70	0,43	0,60	0,70	0,65	0,07	0,40	0,27
Er	0,6	1,8	1,03	-	-	-	0,60	1,90	1,22	1,70	1,90	1,78	0,07	1,00	0,58
Tm	0,07	0,3	0,15	-	-	-	0,07	0,30	0,16	0,20	0,20	0,20	0,07	0,10	0,08
Yb	0,6	7	2,48	7	7	7,00	0,60	7,00	2,55	1,40	7,00	3,37	0,07	0,90	0,35
Lu	0,07	0,4	0,17	-	-	-	0,07	0,30	0,14	0,20	0,20	0,20	0,07	0,10	0,07
Y	3,1	13,2	6,59	7	7	7,00	3,10	12,80	7,81	7,00	12,20	10,00	1,20	7,80	4,64
Cs	0,07	0,07	0,07	-	-	-	0,07	1,30	0,29	0,07	0,10	0,09	0,07	0,10	0,07
Ta	0,35	5	1,64	-	-	-	0,35	2,00	0,78	0,35	1,00	0,51	0,35	0,35	0,35
Hf	0,35	3	1,84	-	-	-	0,35	4,00	2,44	2,00	3,00	2,25	2,00	4,00	3,00
Ag	0,7	0,7	0,70	-	-	-	0,70	0,70	0,70	0,70	0,70	0,70	0,70	0,70	0,70
Bi	3,5	16,801	9,79	-	-	-	13,42	36,43	20,09	16,51	18,64	18,05	0,35	20,16	11,23
Li	3,5	3,5	3,50	-	-	-	3,50	3,50	3,50	3,50	3,50	3,50	3,50	3,50	3,50
Se	7	7	7,00	-	-	-	7,00	7,00	7,00	7,00	7,00	7,00	0,70	7,00	1,15
Sn	3,5	3,5	3,50	-	-	-	3,50	3,50	3,50	3,50	3,50	3,50	3,50	3,50	3,50
Ti	14	14	14,00	-	-	-	14,00	14,00	14,00	14,00	14,00	14,00	1,40	14,00	2,30
Au	1,4	1,4	1,40	-	-	-	1,40	1,40	1,40	1,40	1,40	1,40	1,40	395,00	56,67
Cd	0,07	0,1	0,07	-	-	-	0,07	0,10	0,08	0,07	0,07	0,07	0,07	0,70	0,15
Ga	1,4	3,9	2,07	-	-	-	0,80	3,30	1,61	1,10	1,20	1,15	0,20	1,60	0,99
In	1,3	3,5	2,07	-	-	-	0,20	0,90	0,56	0,30	0,40	0,33	0,07	2,70	0,97
Sc	0,07	7	1,55	7	7	7,00	0,07	7,00	2,04	0,30	7,00	2,72	0,07	0,50	0,10
Th	1,4	260	50,11	150	160	155,00	1,40	180,00	36,46	1,40	70,00	22,60	1,40	1,40	1,40
Tl	0,14	0,14	0,14	-	-	-	0,14	0,14	0,14	0,14	0,14	0,14	0,14	11,00	2,30
U	1,4	70	13,68	38	39	38,50	1,40	62,00	12,42	2,70	75,00	25,62	1,40	26,90	9,36
As	11	33	19,26	-	-	-	14,00	27,00	18,10	3,00	18,00	9,00	0,35	4,00	1,39
Be	0,35	1	0,41	-	-	-	0,35	5,00	1,14	0,35	1,00	0,84	0,35	0,35	0,35
Cu	1	21	5,64	3,5	3,5	3,50	1,00	5,00	2,42	2,00	4,00	2,83	1,00	18,00	2,79
Ge	0,35	4	1,41	-	-	-	0,35	5,00	1,77	0,35	2,00	0,93	0,35	0,35	0,35
Mo	0,35	1	0,41	-	-	-	0,35	1,00	0,42	0,35	1,00	0,51	0,35	0,35	0,35
Pb	0,35	73	10,92	12	14	13,50	2,00	62,00	28,46	1,00	51,00	15,33	13,00	54,00	34,79
Sb	8	17	13,70	-	-	-	8,00	17,00	12,40	5,00	10,00	7,75	0,35	0,35	0,35
V	7	32	15,69	7	7	7,00	7,00	22,00	15,46	7,00	19,00	13,17	2,00	9,00	3,00

Table 1- Geochemical analyses of the iron deposits in the Mansurlu area (min: mininum value, max: maximum vale, mean: aritmetic mean) (cont.).

	Menteşdere Iron Deposit			Karaköy drilling			Attepe Iron Deposit	Demirçoluğu creek	Kartalkaya Iron Deposit
	hematite+goethite n=5			hematite+goethite n=8			hematite+goethite n=1	siderit n=1	hematite+goethite n=1
	min.	max.	mean	min.	max.	mean			
%									
SiO_2	1,20	2,60	1,80	1,80	22,60	6,93	7,7	3	2,5
TiO_2	0,07	0,07	0,07	0,07	0,20	0,09	0,07	0,07	0,07
Al_2O_3	0,07	0,20	0,15	0,20	4,30	1,14	0,3	0,1	0,2
Fe_2O_3	77,30	85,10	81,60	42,60	61,10	54,49	80,3	60,2	73,9
MnO	1,30	1,90	1,58	0,60	1,00	0,81	1,3	0,07	1,2
MgO	0,10	0,40	0,28	0,10	0,80	0,45	0,4	3,2	0,4
CaO	0,10	7,20	2,94	0,10	0,50	0,23	1,4	0,9	6,1
Na_2O	0,07	0,07	0,07	0,07	0,07	0,07	0,07	0,07	0,07
K_2O	0,07	0,07	0,07	0,07	0,80	0,22	0,07	0,3	0,07
P_2O_5	0,07	0,20	0,10	0,07	0,10	0,07	0,07	0,07	0,07
A.Z.	10,35	12,00	11,46	7,95	16,40	10,88	8,19	31,88	15,4
ppm									
Ba	1000,00	2500,00	1700,00	70,00	54100,00	6952,50	1365	70	7000
Rb	7,00	7,00	7,00	-	-	-	10,5	10,5	7
Sr	7,00	42,00	19,20	70,00	800,00	161,25	10,5	10,5	102
Zr	-	-	-	-	-	-	21	21	
Nb	7,00	7,00	7,00	-	-	-	-	-	7
Ni	3,50	12,00	5,20	-	-	-	21	21	30
Co	7,00	10,00	7,60	-	-	-	210	210	60
Zn	35,00	82,00	53,20	-	-	-	79	69	149
Cr	7,00	7,00	7,00	-	-	-	42	42	16
La	7,00	7,00	7,00	-	-	-	-	-	7
Ce	-	-	-	-	-	-	-	-	-
Pr	-	-	-	-	-	-	-	-	-
Nd	21,00	24,00	22,60	-	-	-	-	-	30
Sm	-	-	-	-	-	-	-	-	-
Eu	-	-	-	-	-	-	-	-	-
Gd	-	-	-	-	-	-	-	-	-
Tb	-	-	-	-	-	-	-	-	-
Dy	-	-	-	-	-	-	-	-	-
Ho	-	-	-	-	-	-	-	-	-
Er	-	-	-	-	-	-	-	-	-
Tm	-	-	-	-	-	-	-	-	-
Yb	7,00	7,00	7,00	-	-	-	-	-	7
Lu	-	-	-	-	-	-	-	-	-
Y	7,00	7,00	7,00	-	-	-	-	-	7
Cs	-	-	-	-	-	-	-	-	-
Ta	-	-	-	-	-	-	-	-	-
Hf	-	-	-	-	-	-	-	-	-
Ag	-	-	-	-	-	-	-	-	-
Bi	-	-	-	-	-	-	-	-	-
Li	-	-	-	-	-	-	-	-	-
Se	-	-	-	-	-	-	-	-	-
Sn	-	-	-	-	-	-	-	-	-
Ti	-	-	-	-	-	-	-	-	-
Au	-	-	-	-	-	-	-	-	-
Cd	-	-	-	-	-	-	-	-	-
Ga	-	-	-	-	-	-	-	-	-
In	-	-	-	-	-	-	-	-	-
Sc	7,00	7,00	7,00	-	-	-	-	-	7
Th	90,00	210,00	178,00	-	-	-	-	-	190
Tl	-	-	-	-	-	-	-	-	-
U	41,00	67,00	52,80	-	-	-	-	-	45
As	-	-	-	-	-	-	-	-	-
Be	-	-	-	-	-	-	-	-	-
Cu	3,50	3,50	3,50	-	-	-	21	21	26
Ge	-	-	-	-	-	-	-	-	-
Mo	-	-	-	-	-	-	-	-	-
Pb	7,00	28,00	12,80	-	-	-	14	14	41
Sb	-	-	-	-	-	-	-	-	-
V	7,00	7,00	7,00	-	-	-	10,5	16	20

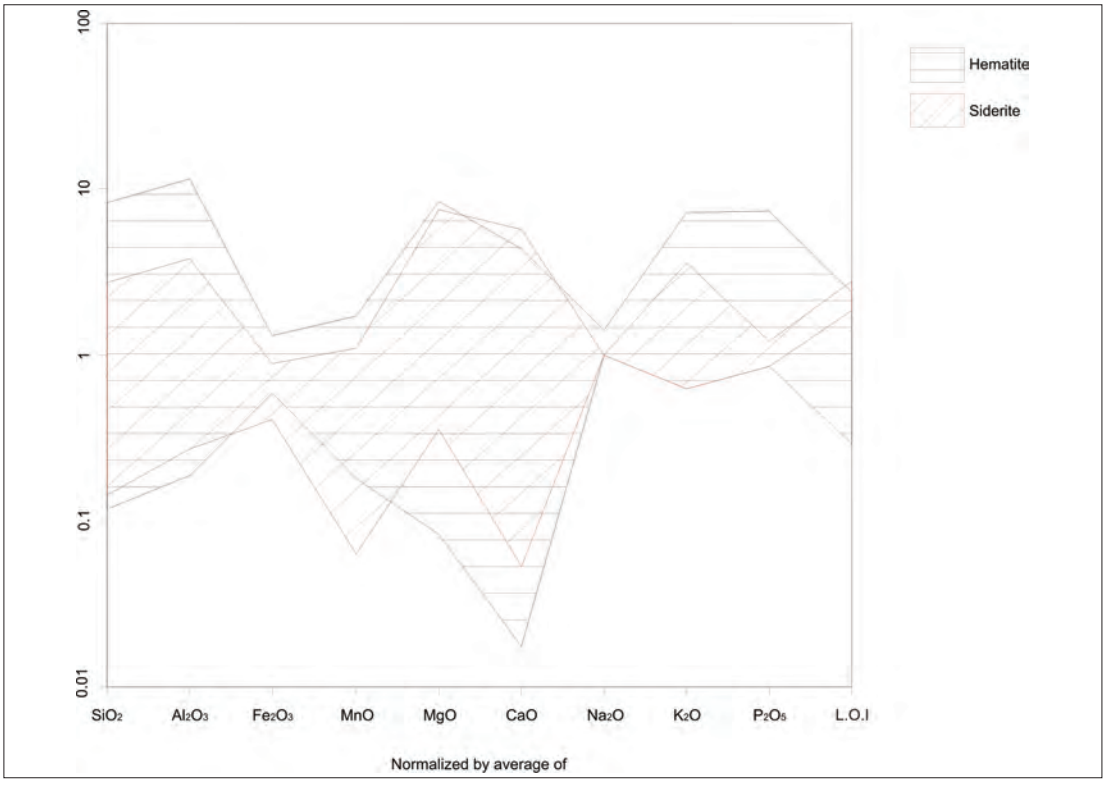

Figure 18- Major-oxides average-normalized diagrams of the hematites and siderites.

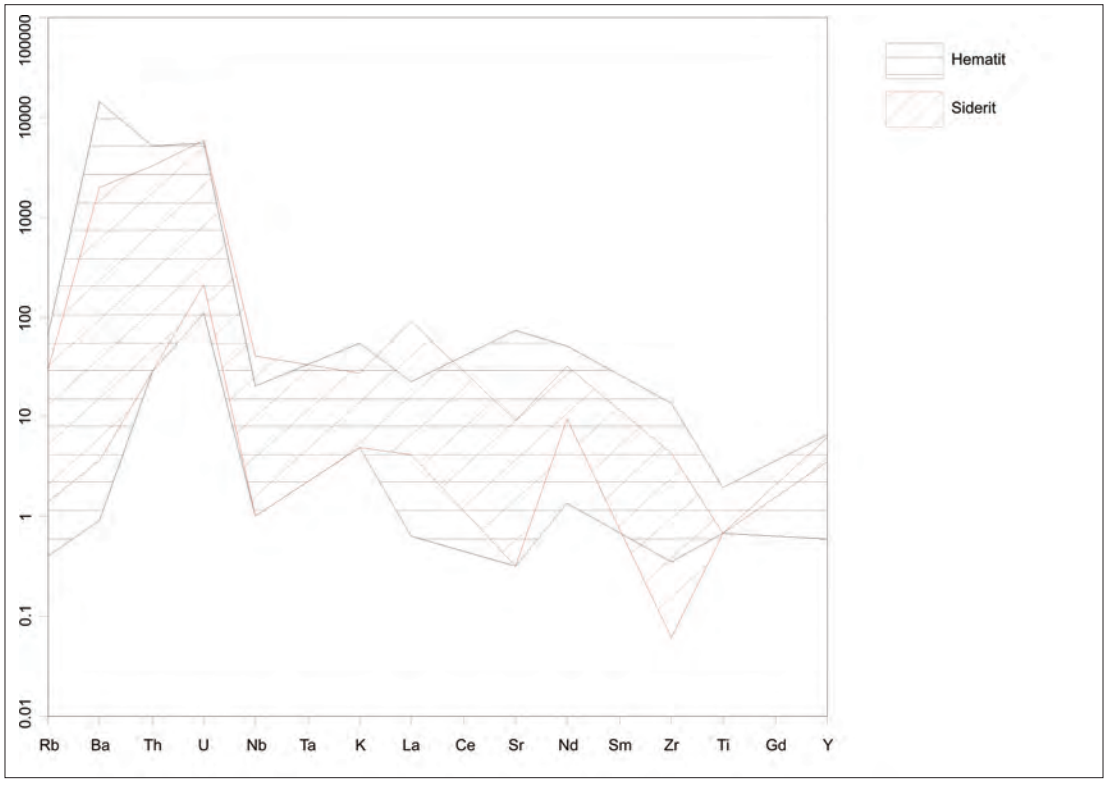

Figure 19- Trace elements chondrite-normalized diagrams of the hematites and siderites (normalization data from Sun et al., 1980).

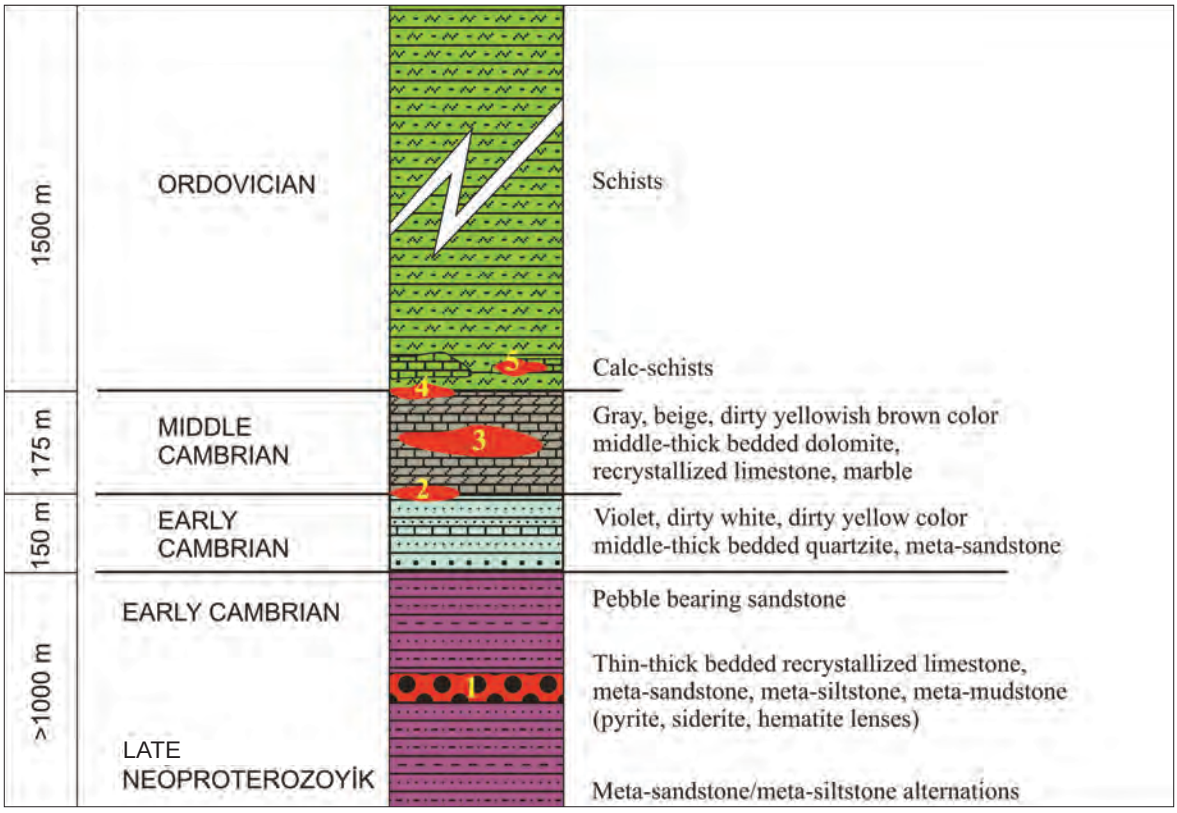

Figure 20- Stratigraphic columnar section of the iron mineralization.

7. Discussion, Correlation and Interpretation

The presence of the bimodal magmatism and rift related basin formed in the back-arc environment was previously discussed based on mineralogical, petrographical, geochemical and geostatistical methods in the earlier studies and in this study (Dayan, 2007; Dayan et al., 2008; Tiringa, 2009; Tiringa et al., 2009). The rift related sequence observed in the Early Cambrian Koçyazı formation in the eastern Taurides can be correlated with similar rock units cropping out in the central Taurides (Gürsu and Göncüoğlu, 2005*a*). Tringa et al. (2009) mentioned that first-stage of the rifting process observed in Sandıklı during the Early Cambrian might have been started during the Late Neoproterozoic period in the Kayseri-Adana Basin. İlinai et al. (2001) proposed a model about duration time of the rifting process and mentioned that the spreading rates in the intra-continental rifting are much higher than back-arc basins as showing the extension in the Arap Plate and opening of the Red Sea that occurred within the last 30 my On the contrary, lithospheric thinning rates in the North Australian Craton was much slower than Arabian Plate and the continental breakdown continued nearly 140 my (Betts et al., 2003). Rapid extensional process is generally associated with the fast increase of the geothermal gradient and genesis of the large volume magmatism (Betts et al., 2003). The limited magmatic products in the studied area and lithological and magmatic correlations with the equivalent units in the Sandıklı (western Taurides) indicate that the back arc rifting process might have been formed during the Late Neoproterozoic to Early Cambrian.

There are different suggestions about the genesis of the iron mineralization in the Mansurlu basin in the previous studies. One part of these studies mentioned that the formation of the iron deposits might be related with the hydrothermal type epigenetic mineral deposits that may be in contact with deep-seated granitic rocks (Henden and Önder, 1980; Küpeli, 1991; Küpeli et al., 2006). However, recent studies suggest a metamorphosed volcanic syn-sedimentary and/or exhalative syn-sedimentary mineral deposit model for the genesis of the iron mineralization (Dayan et al., 2008; Tiringa et al., 2009, 2011). The presence of bimodal volcanism in the studied area also supports the volcanic syn-sedimentary and/or exhalative syn-sedimentary deposit models previously proposed by

the recent studies. Another approach against the other models is that the metals, which are the origin of ores, might have been transported from land into the basin and deposited by the chemical sedimentation.

As a result of subduction of the Proto-Tethys Ocean beneath the Tauride-Anatolide Platform (TAP) in the Late Neoproterozoic, the arc magmatism was developed on the continental margin of the TAP and arc-related basic and acidic volcanics and their tuffs bearing silisiclastic rocks (Emirgazi formation) were deposited at the fore-arc environment (Dayan, 2007; Dayan et al., 2008; Tiringa, 2009; Tiringa et al., 2009; Tiringa et al., 2011). The rifting process was developed in the continental crust by the extensional regime that resulted in the rollback of the subducted Proto-Tethys Ocean during the Early Cambrian (Gürsu and Göncüoğlu, 2005; Gürsu et al., 2015; Gürsu, 2016) (Figure 21a).

The thinning of the continental crust in the preliminary stages of rifting resulted in the genesis of the anatexis granites followed by the formation of the basic and intermediate submarine volcanic rocks and its derivatives along the fracture zones due to the mantle upwelling processes. They were deposited together with the coeval sediments and formed the volcanosedimentary sequences (Koçyazı formation) in the basin during the Early Cambrian (Figure 21b, c). In this tectonic environment, the areas having different Eh and pH values depending on the topography of the basin will lead to the formation of stratiform and stratabound type mineralizations there (Dayan, 2007; Dayan et al., 2008). The iron ore forming metals are accompanied either by solutions/melts enriched by ionic metals in marine water, which flows down through fractures into depths, then warms up and rises to the submarine environment, or by Fe+2 included melts transported from the basic rocks cropped out in the land by the weathering processes. The solutions enriched with metals by discharging onto the sea bottom, can be deposited as magnetite, siderite and/or hematite and pyrite based on their Eh and pH characteristics.

The diversity of the mineralization and magmatism were directly related with the continuity of the subduction of the oceanic crust and breakoff process (Figure 21d). The succession and mineralizations affected by the active deformational phases and metamorphism processes were exhumed to the surface by the post-mineral faults and denudation processes. These fault zones created suitable environments for the processes of karstification and resulted in the enrichment of the limonites and goethites by the alterations of the primary ore minerals of the siderites and/or hematites. The secondary coarse grain siderites which filled up the fractures cutting the sedimentary siderites in the Attepe Iron Deposits and goethite/limonite rich karstic fills observed in the base of the open-pit mine also support our model proposed above. Similar karst infilling mineralization is widely observed in the Karaçat and Kızıl Iron Deposits. Dayan et al. (2008) emphasized that metals dissolved from primary sedimentary origin iron minerals were formed by the late stage mineralized vein and veinlets, which pass through most of the rocks in the region along the fracture zones.

Iron mineralizations in the study area based on similar volcanic features can be correlated with Lahn-Dill in West-Central Germany, Zamora in Romania, Vares in Yugoslavia, Zarigan-Chahmir in Central Iran in the world and with Deveci Iron Deposit in Turkey. But, the metamorphosed type of exhalative sedimentary iron deposits of BIFs named as "Algoma Type" (Bottke, 1981) also presents similar features of the studied iron deposits.

8. Conclusions

The study area is located within the Mansurlu and Feke slices representing rock units of the Geyikdagi Unit in the Eastern Taurides of the Tauride-Anatolide platform (TAP) and are composed of outcrops of the Late Proterozoic Emirgazi formation, Early Cambrian Koçyazı and Zabuk formations, Middle Cambrian Değirmentaşı formation and Early to Late Ordovician Armutludere formation.

Iron mineralizations in the study area have tectonicaly contacted with host rocks today. The oblique and strike slip faults which had contact with the iron mineralizations were determined in the studied area and the deformational forces that affected the fault systems are concentrated in the NE-SW and NW-SE directions in the studied area.

The hematite-goethite-limonite, siderite-limonite, pyrite-limonite, chromite-magnetite and magnetite-ilmenite alterations and bended/broken parts on the specularites were determined in the ore microscopy. In addition, the rhombohedral forms of the carbonate minerals in the hematite are widespread in the studied area.

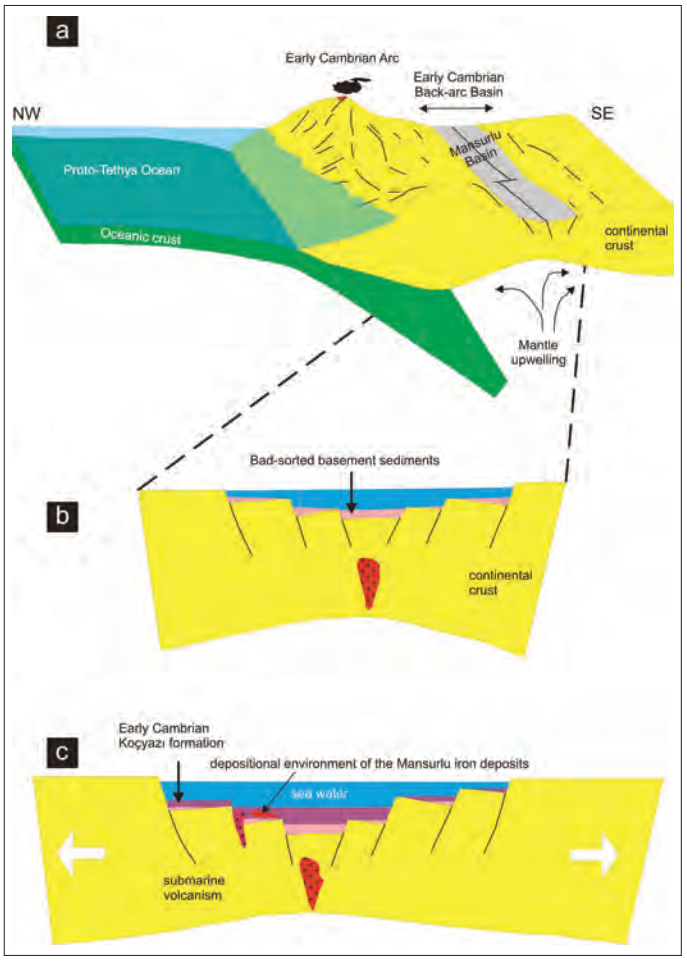

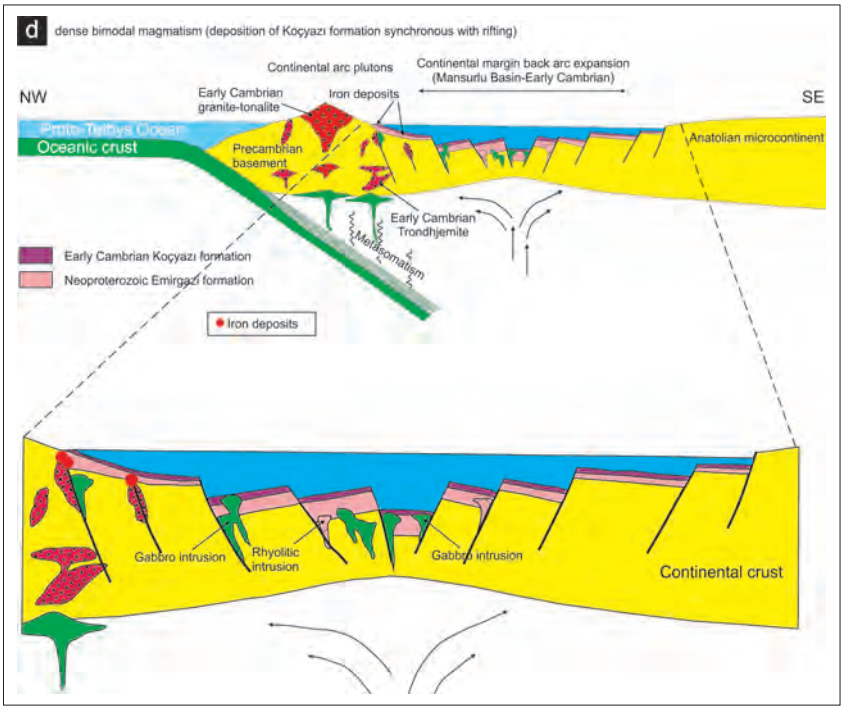

Figure 21- Geodynamic evolution of the genesis of the iron mineralization in the Mansurlu Basin (modified from Gürsu and Göncüoğlu, 2005*b*; Rajabi et al., 2015).

The predominant Ca, Fe, Mn and Mg elements with S, K, Al and Si were determined on the rhombohedral forms of the hematites in SEM analyses. This data indicate that hematite with carbonate forms represent the alteration products of primary siderites.

The multi-elemental patterns of the hematite and siderite samples display similar trends in the major oxides and chondrite normalized trace element diagrams. This result geochemically supports that hematites were derived from the alteration products of primary siderites.

The field and ore microscopy studies show that the main ore minerals are composed of siderite and/or hematite, magnetite and pyrite as primary minerals. They are widely observed within the Late Neoproterozoic Emirgazi formation and Early Cambrian Koçyazı formation, where they are commonly placed within the contact of the sedimentary rocks of the formations. The field observations, ore microscopy, SEM/EDX results combined with the geochemical analyses show that the iron ores representing the late-stage of the mineralization were also formed within the Early Cambrian Zabuk formation, Middle Cambrian Değirmendere formation and Early to Late Ordovician Armutludere formation.

The primary source of the mineralization in the studied area might have been formed from volcanosedimentary-type or exhalative sedimenatary-type (syn-sedimentary) deposits and the mineralization later have undergone metamorphism and tectonic events to exhume to the recent position.

Acknowledgement

This study is the summary of PhD thesis of the first author under the supervisor of the second author at the Graduate School of Natural and Applied Sciences, Department of Geological Engineering of Ankara University. The authors thank to Şükrü Koç (Ankara University) for his contributions during ore microscopy studies, Okan Delibaş (Hacettepe University) for constructive comments and Emmanuel D. Sunkari for linguistic editing. The anonymous reviewers are acknowledged and improved the paper.

References

Arda, N., Tiringa, D., Ateşçi, B., Akça, A., Tufan, E. 2008. Yahyalı (Kayseri)-Mansurlu (Feke-Adana) Yöresi Demir Sahaları Maden Jeolojisi Ara Raporu. *Maden Tetkik ve Arama Genel Müdürlüğü Rapor No: 44437,* 75 s., Ankara (unpublished).

Arıkan, Y. 1966. Adana İli, Kozan ve Feke İlçeleri Demir Zuhurları Hakkında Ön Rapor. *Maden Tetkik ve Arama Genel Müdürlüğü Rapor No: 859,* Ankara (unpublished).

Arıkan, Y. 1968. Mansurlu Demir Zuhurları (Feke-Yahyalı; Adana-Kayseri). *Maden Tetkik ve Arama Genel Müdürlüğü Rapor No: 410,* Ankara ((unpublished).

Betts, P. G., Giles, D., Lister, G. S. 2003. Tectonic Environment of Shale Hosted Massive Sulfide Pb-Zn-Ag Deposits of Proterozoic Northeastern Australia. *Economic Geology,* 98, 557-576.

Bottke, H. 1981. Lagerstattenkunde des Eisens. *Verlag Glückauf GmbH,* Essen, 202.

Brennich, G. 1961. Türkiye'de Demir Cevheri Zuhuratı. *Maden Tetkik ve Arama Genel Müdürlüğü Rapor No:3440*, Ankara (unpublished).

Bubenicek, L. 1964. L'Oxydo-réduction en sédimentologie. *Bulletin BRGM*, 4, 1-36.

Cihnioğlu, M., İşbaşarır, O., Ceyhan, Ü, Adıgüzel, O. 1994. Türkiye Demir Envanteri. *Maden Tetkik ve Arama Genel Müdürlüğü yayını,* Ankara.

Çolakoğlu, A. R., Kuru, S. G. 2002. Attepe Demir Yatağı'nda Jeotermometrik Ölçüm Çalışmaları. *Maden Tetkik ve Arama Genel Müdürlüğü Dergisi,* 125, 1-11.

Dağlıoğlu, C., Bahçeci, A. 1992. Adana-Feke-Mansurlu TDÇİ Ruhsat Sahalarının (Attepe, Koruyeri (Mağarabeli) Değerlendirme Raporu. *Maden Tetkik ve Arama Genel Müdürlüğü Rapor No: 9339,* Ankara (unpublished).

Dağlıoğlu, C., Bahçeci, A., Akça, İ. 1998. Attepe, Koruyeri (Mağarabeli), Hanyeri Batısı (TDÇİ Genel Müdürlüğüne Ait) Demir Madenlerinin Değerlendirme Raporu. *Maden Tetkik ve Arama Genel Müdürlüğü Rapor No: 10101,* Ankara (unpublished).

Dayan, S. 2007. Adana-Mansurlu Attepe Civarındaki Demir Yataklarının Jeolojik, Petrografik ve Yapısal Özelliklerinin İncelenmesi. *Ankara Üniversitesi Fen Bilimleri Enstitüsü Yüksek Lisans Tezi, 125,* Ankara (unpublished).

Dayan, S., Ünlü, T., Sayılı, İ. S. 2008. Adana-Mansurlu Attepe Demir Yatağı'nın Maden Jeolojisi. *Jeoloji Mühendisliği Dergisi,* 32, 2, 1-44.

Demirtaşlı, E. 1967. Pınarbaşı-Sarız-Mağara Civarının Jeoloji Raporu. *Maden Tetkik ve Arama Genel Müdürlüğü Rapor No: 1935,* 129, Ankara (unpublished).

Göncüoğlu, M. C. 2010. Introduction to the Geology of Turkey: Geodynamic Evolution of the pre-Alpine and Alpine terranes. *General Directorate of Mineral Researchand Exploration, Monography Series,* 5, 1-66.

Göncüoğlu, M. C., Dirik, K., Kozlu, H. 1997. General Characteristics of pre-Alpine and Alpine Terranes in Turkey: Explanatory Notes to the Terrane Map of Turkey. *Annales Geologique de Pays Hellenique,* 37, 515-536.

Gürsu, S. 2016. A new petrogenetic model for meta-granitic rocks in the central and southern Menderes Massif – W Turkey: Implications for Cadomian crustal evolution within the Pan-African mega-cycle. *Precambrian Research*, 275, 450-470.

Gürsu, S., Göncüoğlu, M. C. 2005*a*. Batı Toroslar'ın (Sandıklı GB'si, Afyon) Geç Neoproterozoyik ve Erken Paleozoyik Yaşlı Birimlerinin Jeolojisi ve Petrografisi. *Maden Tetkik ve Arama Genel Müdürlüğü Dergisi,* 130, 29-55.

Gürsu, S., Göncüoğlu, M. C. 2005*b*. Early Cambrian back-arc volcanism in the Western Taurides, Turkey: Implications for the rifting along northern Gondwanan margin. *Geological Magazine,* 142, 5, 617-631.

Gürsu, S., Möller, A., Göncüoğlu, M. C., Köksal, S., Demircan, H., Köksal, F. T., Kozlu, H., Sunal, G. 2015. Neoproterozoic continental arc volcanism at the northern edge of the Arabian Plate, SE Turkey. *Precambrian Research*, 258, 208-233.

Henden, İ., Önder, E., Yurt, M.Z. 1978. Adana-Kayseri, Mansurlu-Karaköy (Attepe, Elmadağ Beli, Kızıl Mevkii, Menteşdere, Uyuzpınarı) Demir Madenleri Jeoloji ve Rezerv Raporu. *Maden Tetkik ve Arama Genel Müdürlüğü Rapor No: 6394,* Ankara (unpublished).

Henden, İ., Önder, E. 1980. Attepe (Mansurlu) Demir Madeni'nin Jeolojisi. *T*ürkiye *Jeoloji Kurumu Bülteni,* 23, 1, 153-163.

Ilani, S., Harlavan, Y., Tarawneh, K., Rabba, I., Weinberger, R., Ibrahim, K., Peltz, S., Steinitz, G. 2001. New K-Ar Ages of Basalts from the Harrat Ash ShaamVolcanic Field in Jordan: Implications for the Spanand Duration of the Upper Mantle Upwelling Beneath the Western Arabian Plate. *Geology,* 29, 171–174.

Küpeli, Ş. 1986. Attepe (Mansurlu-Feke) Yöresinin Demir Yatakları. *Selçuk Üniversitesi Fen Bilimleri Enstitüsü, Yüksek Lisans Tezi, 111, Konya* (unpublished).

Küpeli, Ş. 1991. Attepe (Mansurlu-Feke) Yöresi Demir Yataklarının Jeolojik, Petrografik ve Jenetik İncelemesi. *Selçuk Üniversitesi Fen Bilimleri Enstitüsü, Doktora Tezi,* 227, Konya (unpublished).

Küpeli, Ş. 1998. Attepe (Mansurlu-Feke-Adana) Yöresi Demir Yataklarının Jeolojisi ve Kökeni. *Cumhuriyet Üniversitesi Mühendislik Fakültesi Dergisi,* Seri A-Yerbilimleri, 15, 1, 101-118.

Küpeli, Ş., Ayhan, A., Karadağ, M. M., Arık, F., Döyen, A., Zedef, V. 2006. Attepe (Feke-Adana) Demir Yataklarındaki Siderit Mineralizasyonunun C, O, S ve Sr İzotop Çalışmaları ve Jenetik Bulgular. *Jeoloji Mühendisleri Odası 59. Türkiye Jeoloji Kurultayı* Bildiri Özleri Kitabı, 143-144, Ankara.

Lucius, M. 1927. Antitoros Silsilesinde Zamantı Suyu ile Göksu Arasında Faraşa Demir Madeni Zuhurunda Yapılan Jeolojik Taharriyet Hakkında Rapor. *Maden Tetkik ve Arama Genel Müdürlüğü Rapor No: 421,* 84, Ankara (unpublished).

Monod, O. 1977. Recherces Geologiques Dans le Taurus Occidentalausud de Beyşehir-Turqie). Thesed'etat, *l'Univ. De Paris sud., Center d'Orsay,* 442, Paris (unpublished).

Önder, E., Şahin, M. 1979. Adana-Feke-Mansurlu (Hanyeri, Çaldağı, Taşlık Tepe, Mursal Tepe, Bahçecik, Çandırlar, Kısacıklı) Demir Sahaları Jeoloji ve Kozan, Saimbeyli İlçeleri Prospeksiyon Raporu. *Maden Tetkik ve Arama Genel Müdürlüğü Maden Etüt ve Arama Dairesi Rapor No: 1636,* Ankara (unpublished).

Özgül, N. 1976. Torosların Bazı Temel Jeoloji Özellikleri Türkiye Jeoloji Kurumu Bülteni, 19, 1, 65-78.

Özgül, N. 1983. Stratigraphy and Tectonic Evolution of the Central Taurides, Tekeli, O. and Göncüoğlu, M. C. (Ed.), *International Symposium on the Geology of the Taurus Belt.* 77-90, Ankara.

Özgül, N.,Kozlu, H. 2002. Kozan-Feke (Doğu Toroslar) Yöresinin Stratigrafisi ve Yapısal Konumu ile İlgili Bulgular. *Türkiye Petrol Jeologları Derneği Bülteni,* 14, 1, 1-36.

Rajabi, A., Canet, C., Rastad, E., Alfonso, P. 2015. Basin evolution and stratigraphic correlation of sedimentary-exhalative Zn-Pb deposits of the Early Cambrian Zarigan-Chahmir Basin, Central Iran. *Ore Geology Reviews,* 64, 328-353.

Sun, S. S. 1980. Lead isotopic study of young volcanic rocks from mid-ocean ridges, ocean islands and island arcs. *Phils. Trans. R. Soc. Lond.,* 297, 179-202.

Şenel, M., Usta, D., Metin, Y., Bedi, Y., Vergili, Ö., Usta, M., Balcı, V., Kuru, K., Tok, T., Özkan, M., K., Kop, A. 2004. Kozan-Tufanbeyli (Adana) Arasındaki Yapısal Birimlerin Jeolojik Özellikleri. *Jeoloji Mühendisleri Odası 57. Türkiye Jeoloji Kurultayı,* Bildiri Özleri, 275.

Tiringa, D. 2009. Kayseri-Yahyalı-Karaköy, Karaçat Demir Yatağının Maden Jeolojisi. *Ankara Üniversitesi Fen Bilimleri Enstitüsü Yüksek Lisans Tezi,* 139, Ankara (unpublished).

Tiringa, D., Ünlü, T., Sayılı, İ. S. 2009. Kayseri-Yahyalı-Karaköy, Karaçat Demir Yatağının Maden Jeolojisi. *Jeoloji Mühendisliği Dergisi,* 33, 1, 1-43.

Tiringa, D., Çelik, Y., Ateşçi, B., Akça, İ., Keskin, S. 2011. Kayseri-Adana Havzası Demir Aramaları ve Menteş Dere (Yahyalı-Kayseri) Ruhsat Sahasının Maden Jeolojisi Raporu. *Maden Tetkik ve Arama Genel Müdürlüğü Rapor No: 11435,* 153, Ankara (unpublished).

Ünlü, T. 2003. Attepe Demir Yatağı'nda Jeotermometrik Ölçüm Çalışmaları Makalesi Üzerine Eleştiri. *Maden Tetkik ve Arama Genel Müdürlüğü Dergisi,* 126, 87-88.

Ünlü, T., Stendal, H. 1986. Divriği Bölgesi Demir Yataklarının Element Korelasyonu ve Jeokimyası (Orta Anadolu-Türkiye). *TMMOB Jeoloji Mühendisleri Odası Dergisi,* 28, 5-19.

Ünlü, T., Stendal, H. 1989. Divriği Bölgesi Demir Cevheri Yatakları'nın Nadir Toprak Element (REE) Jeokimyası (Orta Anadolu-Türkiye). *Türkiye Jeoloji Kurumu Bülteni,* 32, 21-37.

Ünlü, T., Yıldırım, M., Öztürk, M., Dağlıoğlu, C., Kırıkoğlu, G., Hasarı, M. 1984. Feke-Mansurlu Yöresi Demir Yataklarının Oluşum Modeli Hakkında Bir Yaklaşım. *Maden Tetkik ve Arama Genel Müdürlüğü Maden Etüt Demir İzleme Destek 50225/1104,* 3, Ankara (unpublished).